IMEKO International Conference on
Metrology for Archaeology and Cultural Heritage
Lecce, Italy, October 23-25, 2017

Caveat: measurement strategy for ultra-thin metal layers in gold leaf mosaic tesserae by Monte Carlo SEM-EDS micro- and nanoanalysis simulations

Daniele Moro[1], Gianfranco Ulian[1], Giovanni Valdrè[1,*]

[1] *Dipartimento di Scienze Biologiche, Geologiche e Ambientali, Università di Bologna "Alma Mater Studiorum" Piazza di Porta San Donato 1, 40126 Bologna, Italy. Email: *giovanni.valdre@unibo.it*

***Abstract* – A very useful technique that can provide the local composition of a very thin material, such as the metal leaves of mosaic tesserae, is the Scanning Electron Microscopy (SEM) coupled to Energy Dispersive X-ray Spectrometry (EDS). However a careful analytical strategy must be considered when dealing with tesserae samples, because the metal leaf is extremely thin (0.2 – 1 μm), whereas the thickness of the support and the *cartellina* glasses are usually more than three order of magnitude thicker, and many artefacts could arise from the electron and X-Ray scattering in solids and EDS detector – sample configurations and arrangements. In order to optimize the microanalysis strategy of mosaic tesserae, in this work the effects related to the metal leaf thickness, SEM-EDS setup and detector physics were considered, providing results that could be very helpful to researchers involved in this field. Furthermore, this work provides a correct micro-nanoanalytical strategy to obtain an accurate SEM-EDS quantitative analysis also of other ultrathin layers, substrates, composites and powder materials.**

I. INTRODUCTION

Since the first century AD, metal leaf glass tesserae began to be used in wall mosaics and the first known examples have been found in Rome, for example in the *Domus Aurea* [1]. Gold leaf tesserae begun to be extensively used in the Costantinian age (early IV century AD) and, in particular, in the V century AD by the Ostrogoths in Ravenna [2].

The metal leaves were made with gold, silver or their alloys, which were usually obtained from circulating coins, jewelry or refining, and they were hot fixed between two glass layers (a support glass and a covering layer, the latter called *cartellina*). From the archaeological point of view, it would be very interesting to understand when and where the mosaic tesserae were made. Indeed, it is very difficult to precisely date, as criteria based on style and iconography are not adequately accurate for a good chronological attribution. In addition, several works pointed out that the chemical compositions of the support and *cartellina* glasses are not representative of the source (and date) of the tesserae, as the glass was typically remelted from primary producers [3] or from dismantled mosaics [4-6].

Since the main sources used to produce the metal leaf were the circulating gold coins [7], and their alloy composition over the centuries is well known analytically, in principle it would be possible to date the tesserae by comparing the composition of the gold leaf with that of the coinage products. This important knowledge would help understanding if the mosaic tesserae were newly made or if they were reused from earlier dismantled mosaics.

A very useful technique that can provide the local composition of a material, such as the metal leaves of the tesserae, is the Scanning Electron Microscopy (SEM) coupled to Energy Dispersive X-ray Spectrometry (EDS). However, there is a caveat: a very careful analytical strategy must be considered when dealing with tesserae samples, because the metal leaf is extremely thin (0.2 – 1 μm), whereas the thickness of the support and the *cartellina* glasses are usually more than three order of magnitude greater, and many artefacts could arise from the electron and X-Ray scattering in solids and EDS detector – sample configurations and arrangements. Hence, the quantitative SEM microanalysis of the gold leaf conducted using the standard experimental setups (e.g., electron beam energy of around 20 kV) could provide non-representative results, because of the scattering of the electrons (due to the heavy elements, such as Au and Ag) into the sandwiching glasses and detector configuration respect to the sample surface. In order to

optimize the analysis on such different substrates (support glass, metal leaf and *cartellina* glass), a systematic study of the best instrumental setups is required.

Recently, a study by means of Monte Carlo simulations of the thickness and shape effect on SEM-EDS microanalysis was proposed to study thin asbestos fibres [8]. In the present work, a similar approach was proposed to simulate electron transport, X-ray generation and detection in the tessera composite, made up of the support glass, the metal leaf (with specific Au-Ag-Cu contents) and the cartellina glass, taking into account realistic experimental conditions, such as sample geometry, SEM set-up and EDS detector physics. In order to optimize the microanalysis strategy, in this work the effects related to the metal leaf thickness, electron beam energy, electron elastic/anelastic scattering, element ionization threshold levels, X-ray generation/adsorption/ fluorescence and SEM-EDS chamber setups (azimuthal angle of the probe, take-off angle of the sample, position of the electron beam) were considered. The reported results could be very helpful to researchers interested in using this micro-nano analytical technique to provide a detailed and accurate quantitative analysis of mosaic tesserae or similar composite materials.

II. SIMULATION METHODS

A. Monte Carlo methods

The understanding of electron scattering, X-ray generation, absorption and fluorescence is needed to perform accurate quantitative analysis by X-ray spectroscopy. The simulations presented in this work were carried out by means of Monte Carlo modelling of electron transport and X-ray generation and transport (characteristic and Bremmstrahlung) including primary and secondary fluorescence generation. The Monte Carlo method allows the simulations of electrons trajectories and X-rays through the gold leaf of the mosaic tesserae and to a realistic X-ray detector.

The electron trajectory is modelled taking into account the elastic scattering and a continuous energy loss (continuous slowing down approximation) [9]. Three elastic scattering models are used: a basic screened Rutherford model [10], the Mott scattering cross section of Czyzewski and co-workers [11], and the Mott cross section of Jablonski and co-workers [12]. The energy loss is modelled using the Joy-Luo expression [13], which is an empirical modification of the Bethe energy loss equation [14]. The ionisation cross-section is modelled using the expression of Bote and Salvat [15]. The mass absorption coefficients are those of Chantler and co-workers [16], and the fluorescence yields are tabulated experimental values [17].

The electron source is defined as a Gaussian beam. A response function that mimics the energy resolution of an EDS detector is convolved with the emitted X-ray events. The effect the thickness of the gold leaf was evaluated by simulating EDS spectra of a sample. Peak intensities were integrated and compared as a function of thickness, beam energy, and beam and detector position for all the tesserae samples, after background subtraction.

B. Mosaic tesserae models

In the present work, mosaic tesserae models were created to take into account both the gold leaf thickness and the typical composition of the materials (metal leaf, support glass and *cartellina* glass). The chemical composition and mass densities of the investigated tesserae materials are reported in Tables 1 and 2 (the composition is expressed in wt% of oxides for the glass and in wt% of the elements for the gold leaf). The typical material compositions were chosen and selected from literature among previously measured ones [2, 18].

Table 1. Chemical composition (wt% of oxides) of the simulated glass material. Mass density = 2.5 g/cm^3.

SiO_2	Al_2O_3	Na_2O	K_2O	CaO	MgO	SO_3
69.00	2.40	17.00	0.50	7.00	1.00	0.25
P_2O_5	Cl	TiO_2	Fe_2O_3	MnO	Sb_2O_3	
0.15	1.00	0.10	0.60	0.70	0.30	

Table 2. Chemical composition (wt% of the elements) of the simulated gold leaf. Mass density = 19.1 g/cm^3.

Au	Ag	Cu
96.7	3.0	0.3

A three-dimensional model of the tessera was created, placing a gold leaf of thickness 0.2 μm or 1.0 μm sandwiched between two virtually infinite glasses. The combination of glass compositions and gold leaf thicknesses required the realization of four different models. For the sake of an example, Figure 1 reports a 2D section of one of the geometry considered in the present work. The thin metal leaf (green central area) is placed between two thick glass sections (blue areas on the right and left side of the leaf). The electron beam (red vertical line) is focused on the top exposed side of the metal leaf.

For each model, the influence of the SEM-EDS set-up was simulated taking into account realistic experimental conditions. The influence of the gold leaf thickness on the simulated spectrum was investigated

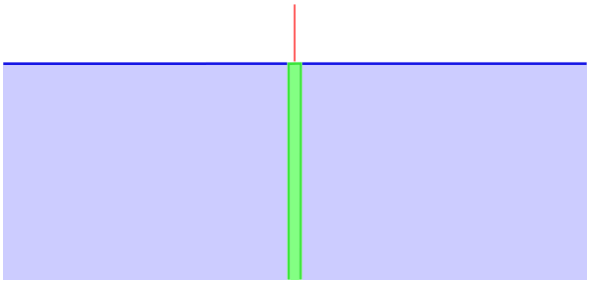

Fig. 1. 2D view of the 3D model of the mosaic tessera.

for electron beam energies of 7.5 keV and 25 keV to better show the effect. An electron probe of 5 nm in diameter was considered.

The probe was focussed in parallel illumination onto the surface of the gold leaf. We simulated two conditions: in the first the probe was centred with respect to the edges of the thin film, and in the second the probe was displaced by 75% of the half width of the gold leaf. These two simulations were performed to assess the effect of the position of the probe with respect to the gold leaf edges. A model of a realistic Si(Li) X-ray detector was employed, accounting for the effect of its performance parameters on the simulated spectra. The modelled EDS detector used to generate the spectrum had an ultra-thin polymer window (Moxtek AP 3.3 film), a gold layer of 7 nm, a dead layer of 10 nm, a detector diode thickness of 3 mm, a sample-to-detector distance of 45 mm, a detector area of 10 mm^2, 4096 channels each of 10 eV and a resolution of 130 eV (FWHM at Mn Kα). In order to investigate the effect of the detector orientation with respect to the direction of maximum extension of the metal leaf, the detector elevation angle was set to 40°, and the effect of the azimuthal angle on the EDS spectrum was investigated by setting this parameter to 0° and to 90°. This means that the gold leaf was oriented with its long axis perpendicular to the detector orientation or in the same direction as the detector, respectively.

III. RESULTS AND DISCUSSION

Several phenomena had to be carefully considered when the dimensions of the object in analysis approach the ones of the electron penetration volume.

In particular, one effect, strongly influenced by the mean atomic number, is related to the elastic scattering of electrons in the finite size of the metal leaf; a second effect is related to the absorption path and fluorescence contribution. Large errors in the quantification can be associated to effects on the generation and measurement of X-rays from a specimen that cannot be considered as a flat polished bulk sample.

Primary characteristic X-ray emission, primary continuum (Bremsstrahlung) emission and secondary fluorescence are considered in the present work. Secondary fluorescence is generated when a primary X-ray (characteristic or continuum) photoionizes an electron from a core shell. It should be noted that secondary fluorescence can come from a material with which the electron beam never interacted, since in most materials the mean free path of energetic X-rays far exceeds the range of electrons.

Figure 2 shows the trajectories of energetic electrons focused on a metal leaf model (the same of Figure 1). In the simulation of the upper image an electron beam of 25 keV and 5 nm Gaussian width (vertical red line), with a probe current of 1nA and a live time of 120 s, was focused on the surface of a 200 nm thick gold leaf in a middle position with respect to the edges. The gold leaf was oriented with its long axis in the same direction as the detector (see the section Simulation Methods for further details). Green trajectories belong to electron scattering inside the metal leaf; blue trajectories are related to electrons in the support glass and *cartellina*; black trajectories belong to electrons escaping the surface of the tessera. The trajectory image clearly shows that, although a 25 keV electron beam contributes to increase the intensity of the measured signal, the energetic electrons scatter out of the 200 nm thick metal leaf travelling for several hundreds of nm sideways through the support glass and cartellina. Clearly a strong contribution to the measured spectrum is expected from the elements of the glass since the volume of interaction greatly exceeds the size of the gold leaf.

In order to confine the signal generation within the thin metal leaf, the energy of the electron beam has to

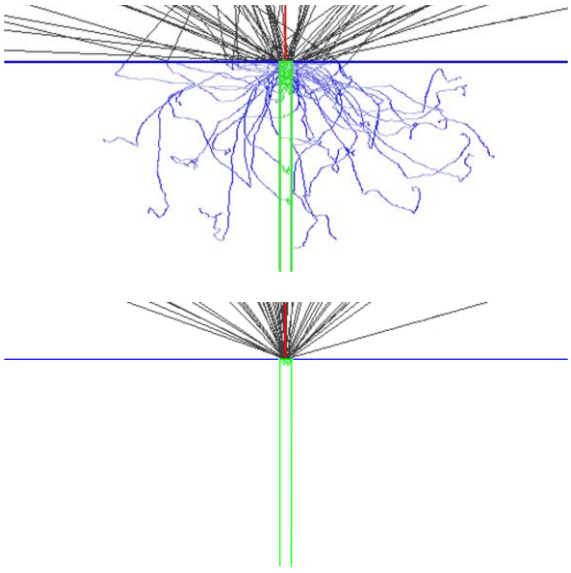

Fig. 2. Trajectories of electron scattering inside a metal leaf of 200 nm and the adjacent support glass and cartellina, for electron beam energy of 25 keV (upper image) and 7.5 keV (lower image).

be lowered, however the incident electron energy should be set up so as to maximize the ionization cross-section for selected shells and elements. The lower image of Figure 2 shows the electron trajectories for the same simulation as the upper image, but with a beam energy of 7.5 keV (about 2.5·Ag Lα). The lower beam energy limits the interaction volume of the electrons in a region roughly comparable to the thickness of the gold leaf.

The EDS spectra resulting from the simulations of figure 2, taking into account X-ray generation (characteristics and Bremmstrahlung), absorption, fluorescence, and detector position, orientation and physics, are shown in Figure 3. The upper spectrum is generated by a 25 keV electron beam, whereas the lower spectrum by a 7.5 keV electron beam. The simulation points out that a beam energy of 25 keV is not suitable for a quantitative analysis of a gold leaf with a thickness of 200 nm, because of the extension of the primary excitation volume (about 6 μm wide), the reduced X-ray generation from the leaf, and secondary fluorescence contribution. The X-ray lines of interest for the Au-Ag-Cu alloy are Au Mα+Mβ, Ag Lα, Cu Kα, in the case of a 25 keV beam.

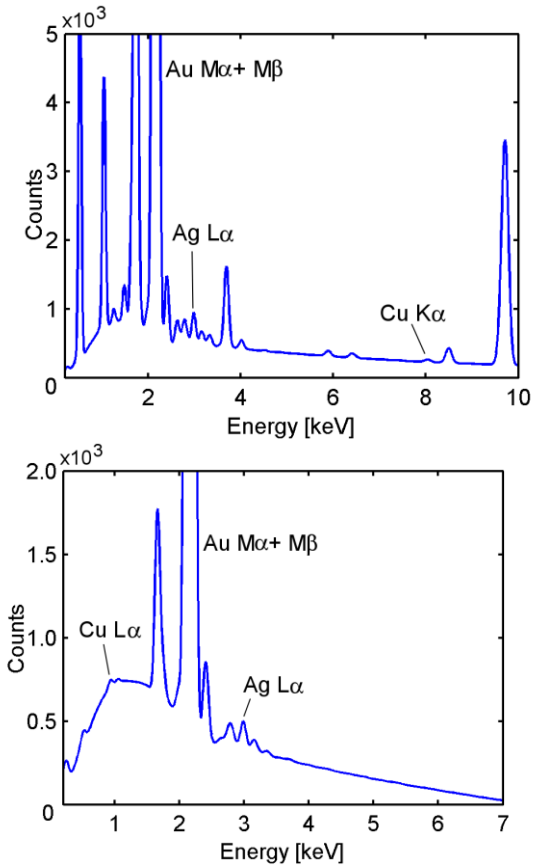

Fig. 3. Simulated EDS spectra as measured by a Si(Li) detector. Upper image: the case of a metal leaf of 200 nm and electron beam energy of 25 keV. Lower image: 200 nm metal leaf and 7.5 keV beam energy.

At 7.5 keV the contribution of the elements of the glass to the spectrum is greatly reduced, but still present (e.g., O Kα, Na Kα, Cl Kα). In this case, the X-ray lines of interest for the Au-Ag-Cu alloy are Au Mα+Mβ, Ag Lα, Cu Lα.

The effects investigated in this work can lead to an inaccurate estimation of the Au-Ag-Cu alloy composition. Figure 4 reports for a comparison the integrated X-ray intensity after background subtraction of a bulk reference sample (dashed line and black stars) as a function of the Au-Ag-Cu alloy composition, in the case of an electron beam energy of 25 keV. The upper image shows the Ag Lα X-ray line integrated intensity, whereas the lower image the Cu Kα line. A 25 keV beam focused on the center of a 200 nm wide gold leaf, with the Si(Li) EDS detector oriented in the same direction as the long axis of the leaf, gives an underestimation of a nominally 3 wt% Ag - 0.3 wt% Cu gold alloy instead to about 2 wt% Ag - 0.14 wt% Cu contents (red cross marker). The quantification

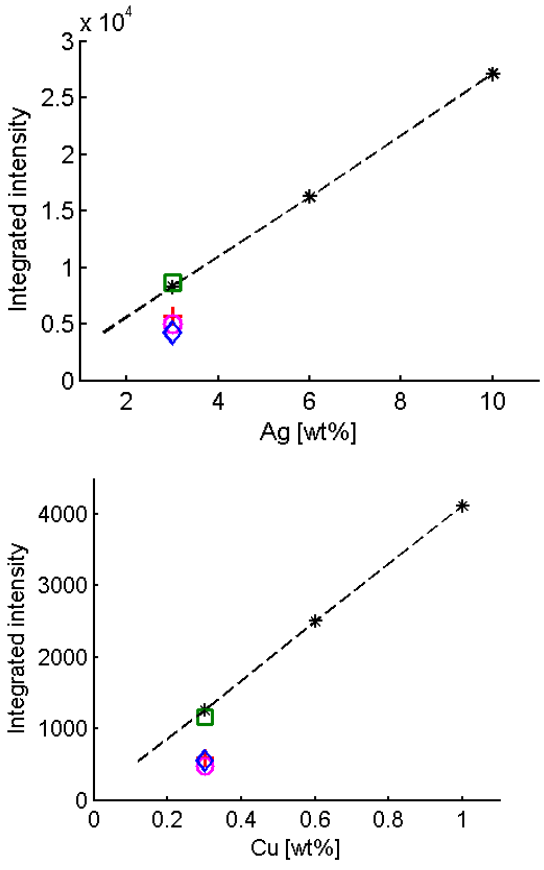

Fig. 4. Simulated reference calibration line for a bulk sample (dashed line and black stars) at beam energy of 25 keV, and integrated intensity for gold leaves of 200 nm and 1 μm taking into account different experimental setups. Upper image: Ag Lα X-ray line. Lower image; Cu Kα.

error can increase if a not centered beam is used (fuchsia open circle): 1.7 wt% Ag - 0.11 wt% Cu. A further contribution to the integrated intensity deviation from the one of a bulk sample is related to the sample-to-detector orientation (azimuthal angle).

A measurement with the detector orientation perpendicular to the long axis of the gold leaf gives an underestimated composition of 1.5 wt% Ag - 0.12 wt% Cu (blue rhombus).

In the case of a thickness of the gold leaf of 1 μm with a 25 keV beam focused in the center and the detector oriented in the same direction as the long axis of the leaf, the interaction volume approaches the leaf thickness and the integrated intensity is near to the reference bulk one (green square marker).

Figure 5 shows the integrated intensity of Ag Lα and Cu Lα peaks obtained focusing a 7.5 keV beam in the center of a 200 nm thick gold leaf with the detector oriented in the same direction as the long axis of the leaf. The integrated intensity are perfectly superimposed to the calibration line for both elements, which indicates a correct setting for accurate quantitative analysis.

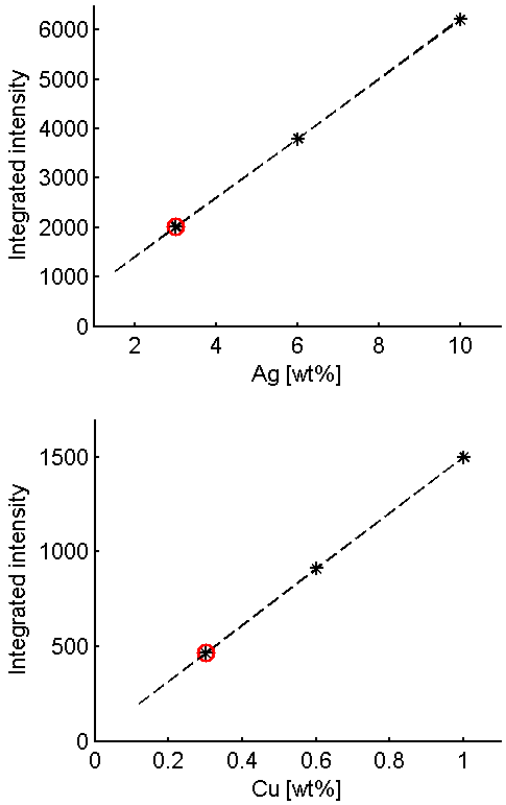

Fig. 5. Simulated reference calibration line for a bulk sample (dashed line and black stars) at beam energy of 7.5 keV, and integrated intensity for a gold leaf of 200 nm (red open circle). Upper image: Ag Lα X-ray line. Lower image; Cu Kα.

IV. CONCLUSIONS

The study presented in this work evidenced the presence of several potential error sources in the quantitative SEM-EDS microanalysis of thin metal leaves of mosaic tesserae, which in turn can affect the dating of the tesserae fabrication. In general the estimation error depends on several factors, such as leaf thickness, electron beam energy and focusing position, sample-to-detector position and orientation, experimental parameters, physical phenomena related to the chemical environment and the specific element considered. A Monte Carlo simulation of a real 3D sample geometry involving both energetic electron trajectory and X-ray generation, absorption, secondary fluorescence, and transport to a realistic EDS detector is advised to plan accurate quantitative SEM-EDS microanalysis of thin specimens.

REFERENCES

[1] H. Lavagne "Le nymphée au Polyphème de la Domus Aurea" Mélanges d'archéologie et d'histoire, 1970, vol. 82, pp. 673-721

[2] E. Neri, M. Verita, I. Biron and M. F. Guerra "Glass and gold: Analyses of 4th-12th centuries Levantine mosaic tesserae. A contribution to technological and chronological knowledge" J. Archaeol. Sci., 2016, vol. 70, pp. 158-71

[3] I. C. Freestone "The provenance of ancient glass through compositional analysis" Mater Res Soc Symp P, 2005, vol. 852, pp. 195-208

[4] A. Cutler "The industries of art" *2002*, in ed. A E Laiou "The Economic History of Byzantium from the Seventh through the Fifteenth Century", vol. 2, pp. 555-87, Washington, USA.

[5] J. DeLaine "The baths of Caracalla. A study in the design, construction, and economics of large-scale building projects in imperial Rome. *" 1997*, Journal of Roman Archeology Supplementary, vol. 25, Portsmouth, Rhode Island, USA.

[6] N. Schibille and I. C. Freestone "Composition, Production and Procurement of Glass at San Vincenzo al Volturno: An Early Medieval Monastic Complex in Southern Italy" PLoS One, 2013, vol. 8,

[7] E. Neri and M. Verita "Glass and metal analyses of gold leaf tesserae from 1st to 9th century mosaics. A contribution to technological and chronological knowledge" J. Archaeol. Sci., 2013, vol. 40, pp. 4596-606

[8] D. Moro and G. Valdre "Effect of shape and thickness of asbestos bundles and fibres on EDS microanalysis: a Monte Carlo simulation" 14th European Workshop on Modern Developments and Applications in Microbeam Analysis (Emas

2015 Workshop), 2016, vol. 109, 012011.
[9] N. W. M. Ritchie "Spectrum Simulation in DTSA-II" Microsc. Microanal., 2009, vol. 15, pp. 454-68
[10] R. Myklebust, D. Newbury and H. Yakowitz "NBS Monte Carlo Electron Trajectory Calculation Program″ *1976*, in ed. K Heinrich, *et al.* "NBS Special Publication", vol. 460, p 105, Washington, DC.
[11] Z. Czyzewski, D. O. Maccallum, A. Romig and D. C. Joy "Calculations of Mott Scattering Cross-Section" J. Appl. Phys., 1990, vol. 68, pp. 3066-72
[12] A. Jablonski, F. Salvat and C. J. Powell 2010 "NIST electron elastic-scattering cross-section database". (Gaithersburg, MD: National Institute of Standards and Technology)
[13] D. C. Joy and S. Luo "An Empirical Stopping Power Relationship for Low-Energy Electrons" Scanning, 1989, vol. 11, pp. 176-80
[14] H. A. Bethe and J. Ashkin "Passage of radiation through matter″ *1953*, in ed. E Segre "Experimental Nuclear Physics", vol. 1, New York, N.Y.
[15] D. Bote and F. Salvat "Calculations of inner-shell ionization by electron impact with the distorted-wave and plane-wave Born approximations" Phys. Rev. A, 2008, vol. 77,
[16] C. T. Chantler, K. Olsen, R. A. Dragoset, J. Chang, A. R. Kishore, S. A. Kotochigova and D. S. Zucker 2005 "NIST Standard Reference Database version 2.1". (Available at http://physics.nist.gov/ffast: National Institute of Standards and Technology)
[17] W. Bambynek, B. Crasemann, R. W. Fink, H. U. Freund, H. Mark, C. D. Swift, R. E. Price and P. Venugopala Rao " X-Ray fluorescence yields, Auger, and Coster-Kronig transition probabilities " Reviews of Modern Physics, 1972, vol. 44, pp. 716-813
[18] A. Conventi, E. Neri and M. Verita "SEM-EDS analysis of ancient gold leaf glass mosaic tesserae. A contribution to the dating of the materials" Iop Conf Ser-Mat Sci, 2012, vol. 32,